The single-particle mechanism behind the asymmetric distortions

Nilsson, Sven Gösta; Larsson, S E; Möller, P

Published in:
Physica Scripta

1974

Physica Scripta. Vol. 10 A, 53–59, 1974

The Single-Particle Mechanism behind the Asymmetric Distortions

S. E. Larsson, P. Möller and S. G. Nilsson

Department of Mathematical Physics, Lund Institute of Technology, Lund, Sweden

Received June 11, 1974

Abstract

The single-particle mechanism behind the asymmetric distortions. S. E. Larsson, P. Möller and S. G. Nilsson (Department of Mathematical Physics, Lund Institute of Technology, Lund, Sweden).
Physica Scripta (Sweden) 10 A, 53–59, 1974.

The relation between nuclear shell structure and nuclear shapes is brought out in diverse mass regions. Thus certain nuclear orbitals, shown to be responsible for the development of mass-asymmetric distortions, are here followed in more detail for large and realistic shape changes. The same holds for axial asymmetries. The study is applied to actinide and superheavy nuclei as well as very light ones, among the latter ^{24}Mg, which is shown to exhibit a deep octupole-shape second minimum.

1. The reflection asymmetric or mass-asymmetric distortions

The connection between shapes and shells is brought out at this conference in the contribution by Bohr and Mottelson [1]. In the spirit of their contribution one may thus ask the question: which shells from which shapes, and conversely: which shapes from which shells? The latter type of question will here be applied to the mass- or reflection-asymmetric degrees of freedom $(P_3 + P_5)$ and the axial-asymmetry angle γ. The explanation of the mass-asymmetry mechanism goes back to the work by Johansson [2]. It has been given a more complete and quantitative formulation in the papers by Möller, Nilsson and Gustafson [3, 4, 5]. From ref. [4] we cite a figure exhibiting single-particle orbitals for given ε ($\varepsilon = 0.85$) and ε_4 ($\varepsilon_4 = 0.12$). It is thus the downbend with asymmetry (Fig. 1) of very specific orbitals just below the Fermi surface that causes the energy gain resulting in a lowering of the second barrier peak by 1–4 MeV for a large region of actinide elements (a result also obtained in the calculations by Strutinsky and Pauli et al. [6], Möller and Nix [7] and Mustafa, Mosel and Schmitt [8]). One may also go one step further and claim that with the inclusion of this degree of freedom a new shell opens at $N \simeq 140$.

The occurrence of a (third) barrier minimum in the theoretical calculations, associated with the neutron number $N \simeq 140$, is then not unexpected. More surprising is the fact that the *same* shell is predicted for the Folded-Yukawa (F.Y.) potential as well as the Modified-Oscillator (M.O.) potential [8]. The third minimum is thus apparent for actinide nuclei with N near 140 for calculations based on both models. A resulting energy surface [5] of ^{232}Th is illustrated in Fig. 2.

The mechanism behind the trend towards asymmetry is brought out in Fig. 3 exhibiting the coupling of orbitals of the type $[Nn_z\Lambda\Omega]$ to $[N+1\, n_z+1\, \Lambda\Omega]$, which orbitals are specifically connected to each other by an operator of the type z or $z(x^2+y^2)$. In fact, of these the $[N0\Lambda\Omega]$-orbitals are the most frequent, most pure and exhibiting the strongest couplings. These orbitals approach each other closely both due to the fact that $\hbar\omega_z$, the fundamental spacing, decreases linearly with ε *and* due to the Y_{40}-term. The latter corresponds physically to the development of a waistline. Indeed, as pointed out by Andersen [9], for a complete waist incision (i.e. at the point of scission) the two mentioned types of orbitals become degenerate in energy. This situation is illustrated in Fig. 4 (from ref. [7]). Without the inclusion of the asymmetry coordinates the $[N0\Lambda\Omega]$ orbitals exhibit a fast rise with ε (which "causes" the initial rise of the second barrier). As the $[N0\Lambda\Omega]$ orbitals approach the Fermi surface, the mentioned octupole type of interaction causes the former orbitals to rise much less steeply with ε due to their mixing with the $[N+1\, 1\, \Lambda\Omega]$ counter-parts. The orthogonal mixture states instead rise even more quickly. For still larger ε they in turn bend because of interaction with the $[N+2\, 2\Lambda\Omega]$ orbitals etc., as can all be studied in Fig. 5.

In the superheavy region the situation with respect to ε_{35} (a notation for $\varepsilon_3 + \varepsilon_5$) deformations shows some resemblance with that encountered for actinides at the second barrier, see Fig. 6. The reason that the resulting reduction due to $P_3 + P_5$ of the outer barrier is so small, is the fact that the barrier distortion in terms of ε and ε_4 is much smaller than in the actinide case. As a result the interacting orbitals at these distortions occur more distant from one another. In turn the shell effect is much smaller. In addition, the liquid drop has a much larger stabilising effect with respect to asymmetric distortions at these smaller ε-values.

The effect of asymmetric distortions on proton levels in the superheavy region is illustrated in Fig. 7 (for $\varepsilon = 0.50$ and $\varepsilon_4 = 0.03$).

It is interesting to survey the periodic table for regions likely to exhibit large effects of octupole asymmetry in addition to the actinide and superheavy regions. It turns out that light nuclei appear especially promising. As these species represent a particularly inappropriate region at this conference, we touch very briefly on the results of the calculations by Leander and Larsson [10] applied to the potential-energy surface of ^{24}Mg (Fig. 8). In the energy surface in an $(\varepsilon, \varepsilon_3)$-plane the octupole deformation minimum is found situated in the lower-right corner of the diagram. The corresponding single-particle level diagram, which explains the mechanism for the formation of this second ^{24}Mg minimum and reminds very much of Fig. 1, is shown in Fig. 9.

2. The deformation of axial asymmetry

We turn now to the problem of the effects of axial asymmetry on the fission barrier. The earliest calculations are here due to Pashkevich [11], whose results have been confirmed by the more detailed calculations by Larsson, Ragnarsson and Nilsson [12] for the M.O. potential, and by Götz et al. [13] for a Woods-Saxon type potential. A recent, much improved calculation, where the effects of γ and ε_4 on the Coulomb energy for the first time are treated consistently, is due to Larsson and Leander [14]. The

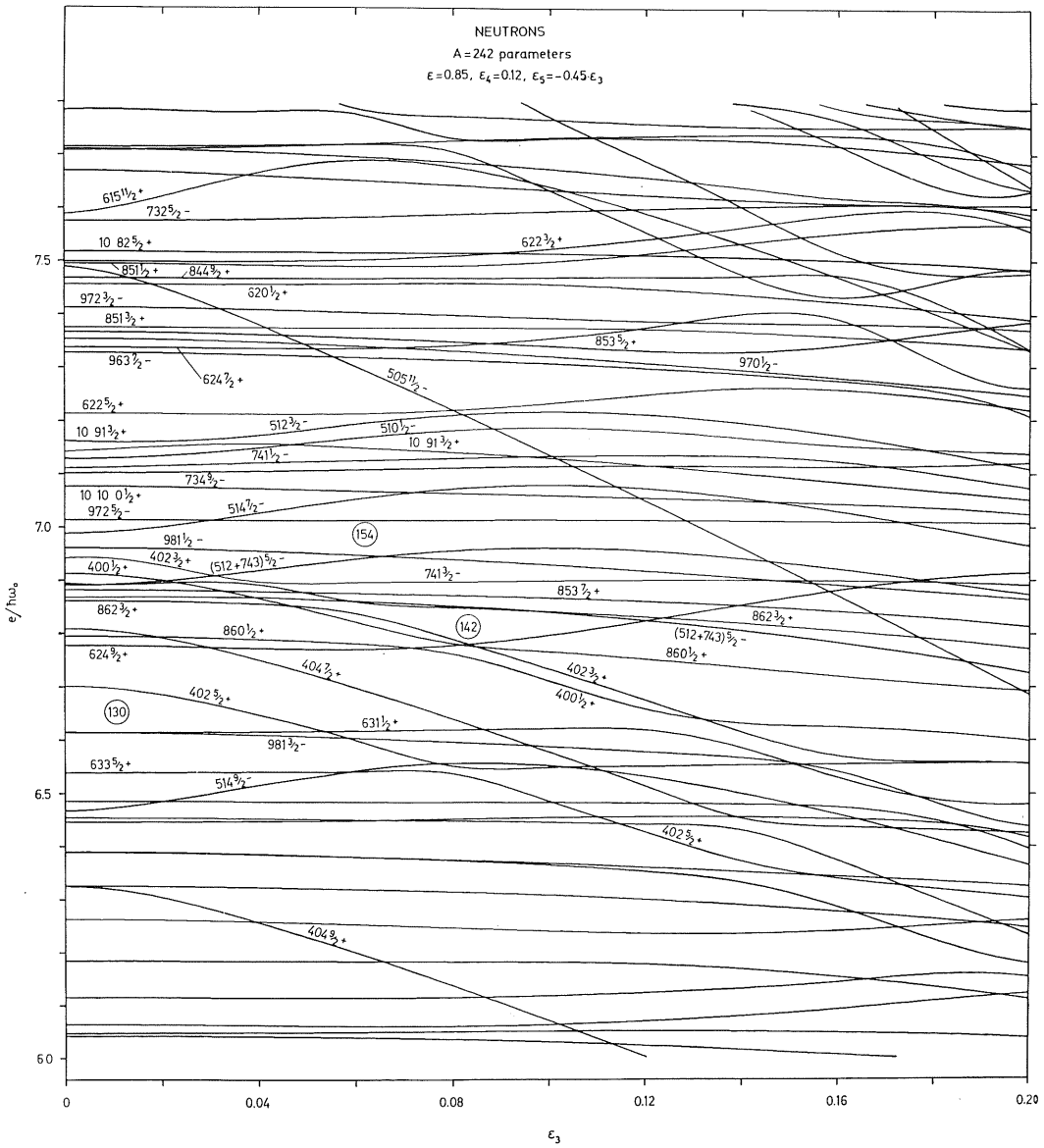

Fig. 1. Single-neutron orbitals in the actinide region for a distortion in ε and ε_4 appropriate to the second-saddle region ($\varepsilon = 0.85$, $\varepsilon_4 = 0.16$) as functions of the mass-asymmetry coordinate ε_3 (and ε_5). Note the strong downward bend of orbitals as [400 1/2], [402 3/2], [402 5/2], [404 7/2], [404 9/2], [505 11/2] etc. These orbitals are found to interact with respectively [510 1/2], [512 3/2] etc ... For a large enough ε_3-value a shell gap is achieved at $N \simeq 140$.

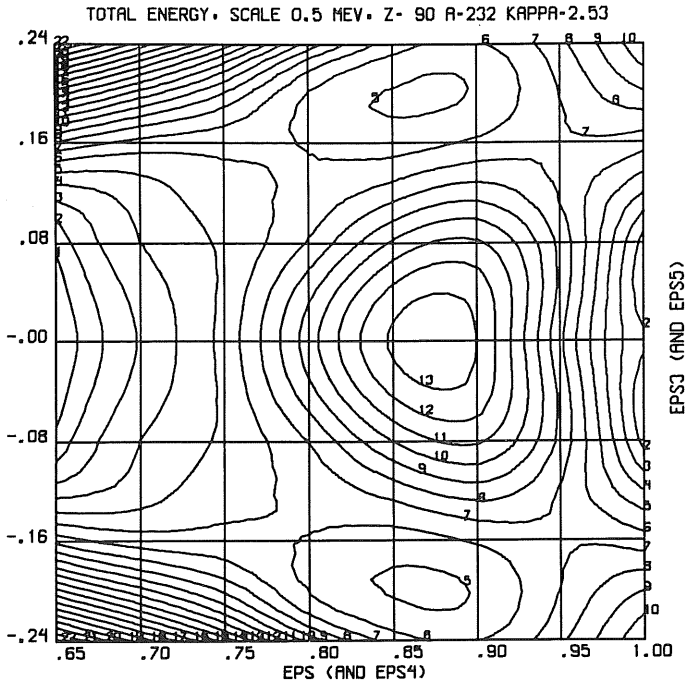

Fig. 2. The potential-energy surface (corresponding to $G = \text{const.}$) for $^{232}_{90}\text{Th}_{142}$ as a function of the elongation ε (and waist-line coordinate ε_4) on the x-axis and the mass asymmetry coordinate ε_3 (and ε_5) on the y-axis. Note the ternary minimum. Fig. taken from ref. [4].

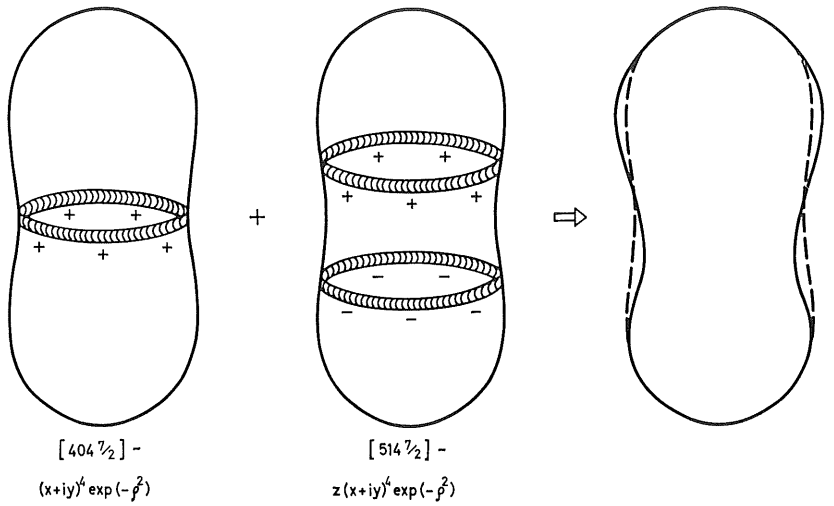

Fig. 3. Discussion of the mechanism of octupole coupling. The "waistline orbital" [404 9/2] with the wave function proportional to $(x+iy)^4 e^{-\varrho^2/2}$, is depicted as a belt around the nuclear waist. It couples via an $r^3 Y_{30}$ type of deformation field in particular to the "double-belt-orbital" [514 9/2], proportional to $z(x+iy)^4 e^{-\varrho^2/2}$, which latter is depicted as two displaced belts, one on each side of the nuclear waist. By mixing with this latter state the "waistline state" moves in a way as seen to the right in the figure.

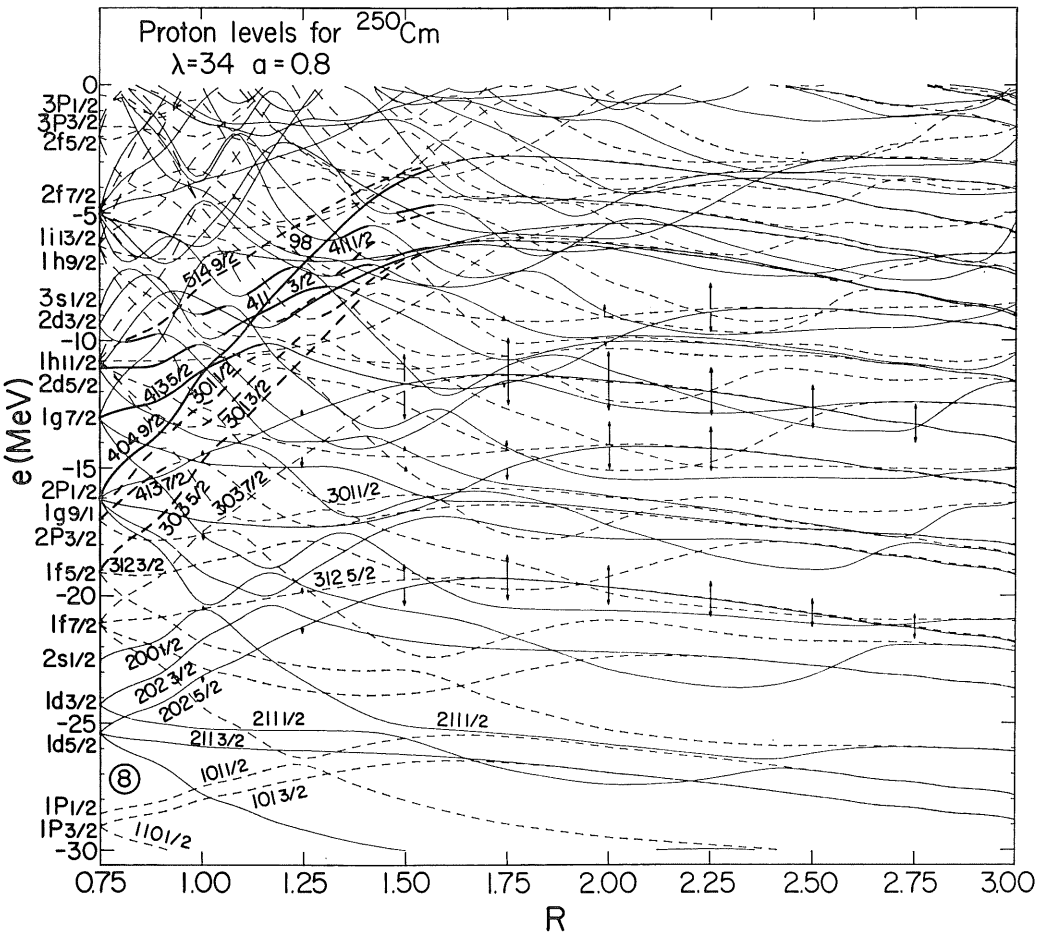

Fig. 4. The single-proton orbitals of the Folded-Yukawa model are plotted all the way to scission. The coordinate used corresponds to the dynamical liquid-drop path. Note the approaching degeneracy of orbitals of the type [211 1/2] and [101 1/2] etc as the waist-line incision becomes complete. Fig. taken from ref. [7].

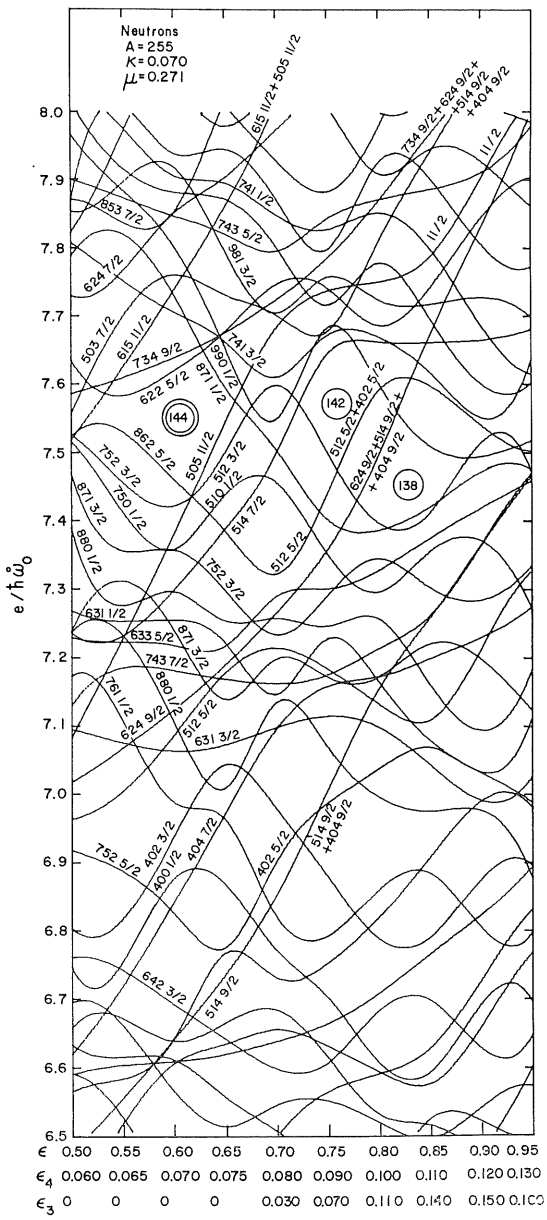

Fig. 5. Single-neutron orbitals (in the M.O. model) as function of elongation and associated mass asymmetry ε (and ε_3). Note that the rapid rise with distortion is temporarily checked by the octupole coupling.

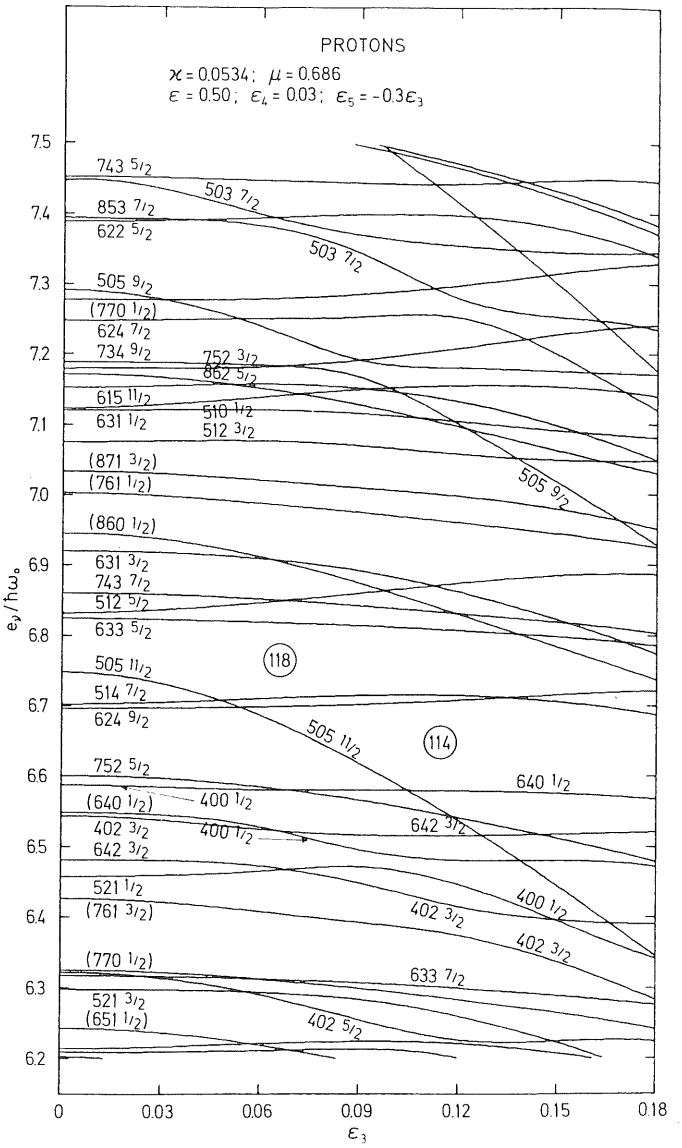

Fig. 7. The single-proton orbitals in the SHE region for saddle point ε and ε_4 distortions as functions of the mass asymmetry coordinate.

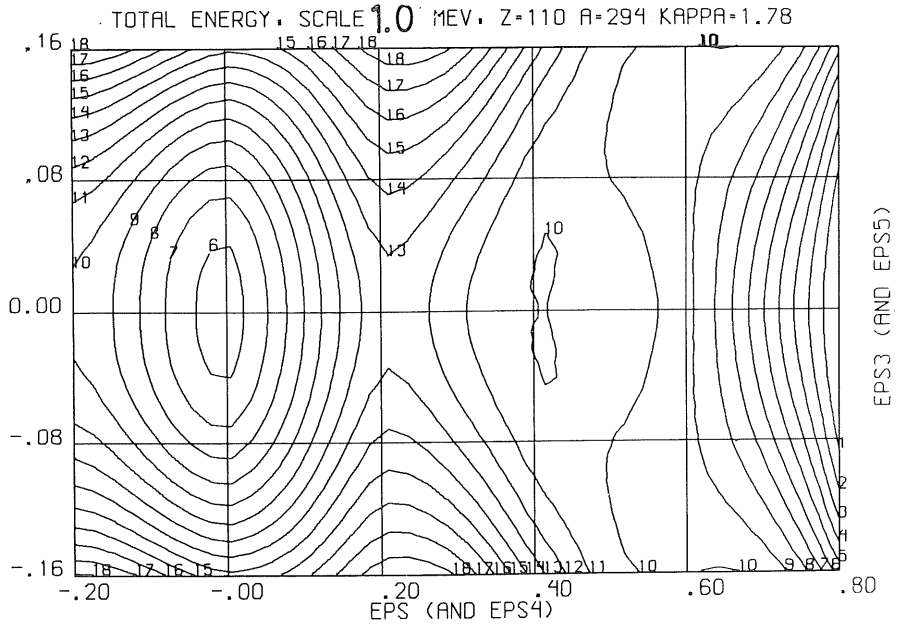

Fig. 6. The potential-energy surface of $^{294}110$ in ε (and ε_4) vs. ε_3 (and ε_5) in the M.O. model. Note the mass-asymmetry of the second barrier.

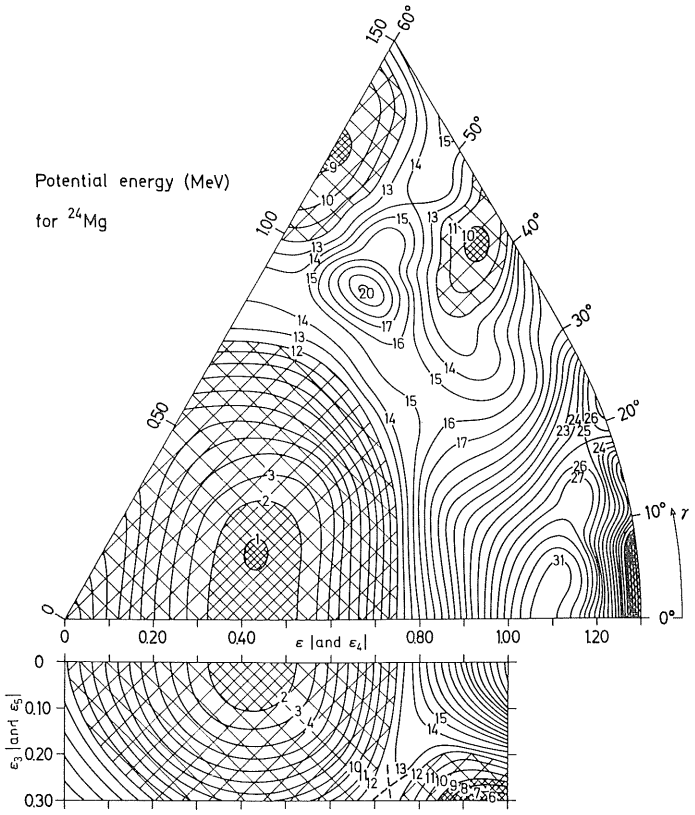

Fig. 8. The potential-energy surface of ^{24}Mg based on the M.O. potential ($\varkappa=0.08$, $\mu=0.1$) and the modified-liquid-drop macroscopic energy (ref. [18]). The upper part is a diagram in ε (and ε_4) vs. γ while in the lower part the space ε vs. ε_3 (and ε_5) is investigated for $\gamma=0$. Note the deep secondary minimum at $\varepsilon=1.0$, $\varepsilon_3=0.3$. This is a shape even more asymmetrically distorted than that corresponding to the actinide second-saddle shapes.

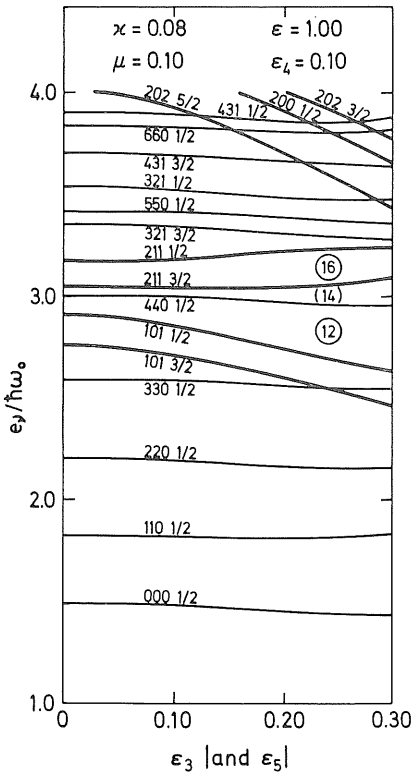

Fig. 9. The single-particle orbitals responsible for the mass-asymmetric shell structure associated with $Z=N=12$. The ε-coordinate is assumed to equal 1.0. Note the great similarity with Fig. 1.

driving force causing instabilities to γ-asymmetry involves orbitals of the type $[Nn_z\Lambda\Omega]$ coupling by $\varrho^2(Y_{22}+Y_{2-2})$ to $[Nn_z\Lambda\pm2\Omega\pm2]$.

In fact, the group of orbitals decisive for the development of γ-instability are partly the same as those involved in the mass asymmetry case, namely the $[N0\Lambda\Omega]$ orbitals. In the γ-instability problem we are concerned with couplings between different orbitals within this one group. This is apparent in Fig. 10, showing the neutron orbitals at $\varepsilon=0.40$ and $\varepsilon_4=0.04$ in the actinide region as functions of γ($\gamma=0°$ to 18°). It appears that a particularly large shell effect is associated with $N=150$ in the actinide region.

One should note that the orbitals interacting via $\varrho^2 Y_{22}$ do not approach each other with increasing ε or ε_4. It is therefore not surprising that the γ-instability usually affects already the ground-state minimum or the first barrier peak.

In the SHE region the most important orbitals affecting the first barrier peak are the proton orbitals, as displayed in Fig. 11. This figure depicts proton orbitals at $\varepsilon=0.25$ (and $\varepsilon_4=0.02$) as a function of the asymmetry angle ($\gamma=0°$ to 30°). The relevant couplings are marked by arrows. The increasing shell effect as Z approaches 114 is apparent.

A detailed deformation energy surface for ^{298}114 is given in Fig. 12 in terms of ε and ε_4. This is a similar picture to the one published by Nilsson, Tsang et al. in 1969 [15] with the difference that the

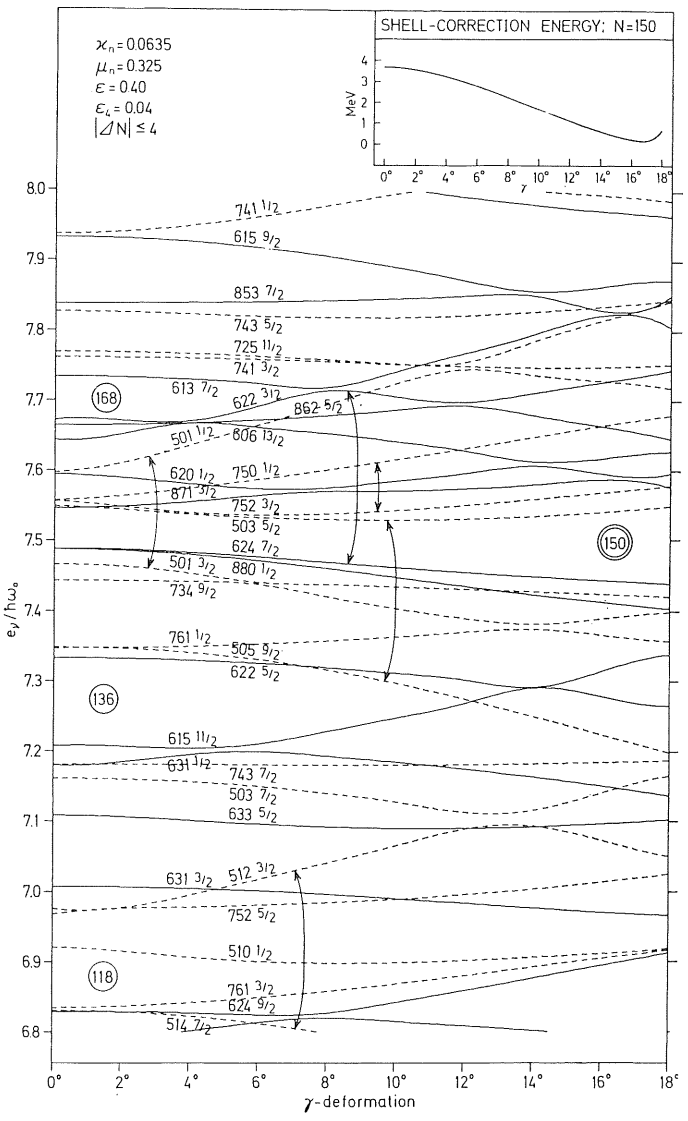

Fig. 10. The single-neutron orbitals in the actinide region (M.O. potential) for the first-saddle point distortions $\varepsilon=0.40$, $\varepsilon_4=0.04$ as functions of γ. The strongly interacting orbitals are connected by arrows.

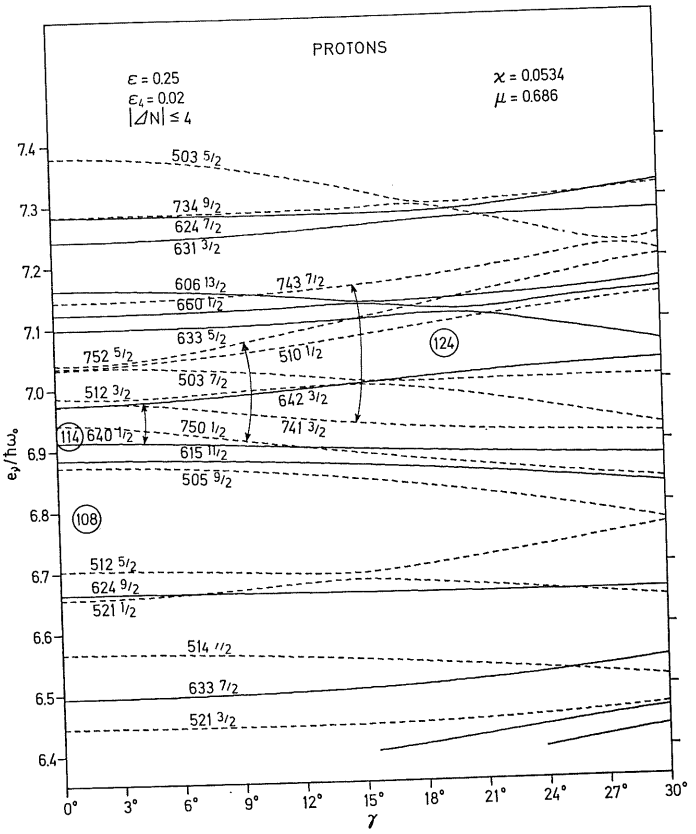

Fig. 11. The single-proton orbitals (M.O. potential) for the first saddle point distortion (in the SHE region) as functions of γ. Interactions are marked by arrows.

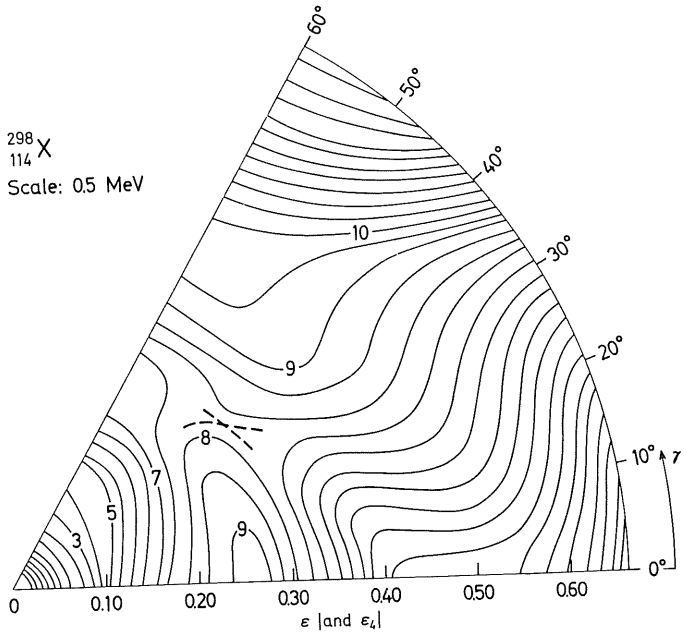

Fig. 13. Same as Fig. 12, but for ε (and ε_4) vs. γ.

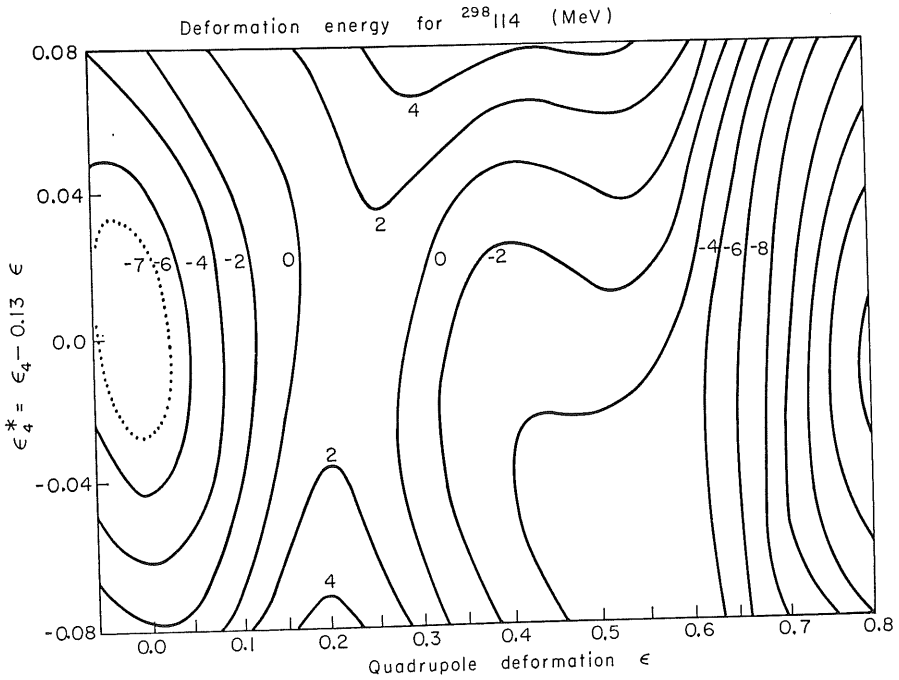

Fig. 12. The potential-energy surface for $^{298}114$ for the M.O. potential combined with the droplet model. The deformation coordinates are ε and $\varepsilon_4^* = \varepsilon_4 - 0.13\,\varepsilon$.

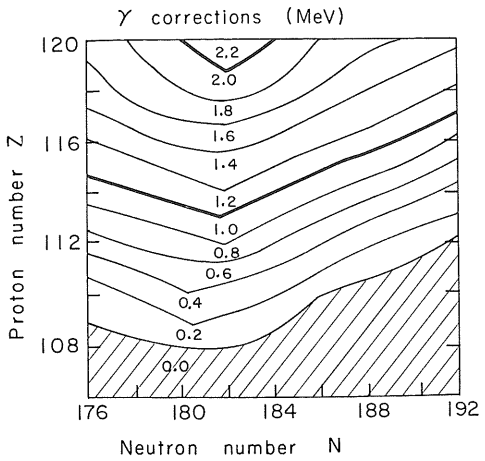

Fig. 14. Contour plot of barrier reduction ΔE_γ, due to γ, as a function of N and Z.

droplet model [16] is used here to generate the "macroscopic" energy surface. The discrepancy with the earlier result is insignificant. The diagram of Fig. 12 is used for a minimisation of the energy surface with respect to ε_4 for each ε-value. In Fig. 13 (from ref. [14]), which is the more interesting figure valid for $^{298}114$, γ is introduced as a variable in addition to ε (and ε_4). The resulting barrier with respect to the ground state minimum, with 0.5 MeV zero-point energy included, is 7.7 MeV. For the nucleide $^{294}110$, the most favourable candidate for long-time survival, all decays considered, the resulting barrier is 5.8 MeV when γ is included.

A diagram exhibiting the energy reduction of the first barrier due to the γ-degree of freedom is shown in Fig. 14. This effect is taken into account in the calculation of the half-lives in another contribution to this conference by the Berkeley–Lund–Warsaw group [17].

The inclusion of $(P_3 + P_5)$ and γ both serve to lower the SHE barriers. The corresponding quantitative results have been reviewed here. Two possible opposing effects, both tending to increase the barriers, namely the Coulomb contribution from the non-homogeneity of the charge distribution and the non-isotropy of the basic pairing correlation matrix element, are considered in the contribution to this conference by the Lund–Berkeley group [19].

Acknowledgement

The authors wish to thank G. Leander for kindly supplying his results prior to publication.

References

1. Bohr, A. and Mottelson, B. R., Contribution to this Symposium.
2. Johansson, S. A. E., Nucl. Phys. **22**, 529 (1961).
3. Möller, P. and Nilsson, S. G., Phys. Lett. **31B**, 283 (1970).
4. Gustafson, C., Möller, P. and Nilsson, S. G., Phys. Lett. **34B**, 349 (1971).
5. Möller, P., Nucl. Phys. **A192**, 529 (1972).
6. Pauli, H. C., Ledergerber, T. and Brack, M., Phys. Lett. **34B**, 264 (1971); Brack, M., Damgaard, J., Stenholm-Jensen, A., Pauli, H. C., Strutinsky, V. M. and Wong, C. Y., Rev. Mod. Phys. **44**, 320 (1972).
7. Möller, P. and Nix, J. R., Los Alamos Preprint LA-UR-74-417, to be published in Nucl. Phys., and references quoted therein; Bolsterli, M., Fiset, E. O., Nix, J. R. and Norton, J. L., Phys. Rev. **C5**, 1050 (1972).
8. Mustafa, M. G., Mosel, U. and Schmitt, H. W., Phys. Rev. **C7**, 1519 (1973).
9. Andersen, B. L., Phys. Lett. **42B**, 307 (1972).
10. Leander, G. and Larsson, S. E., Nuclear Physics, in press.
11. Pashkevich, V. V., Nucl. Phys. **A133**, 400 (1969).
12. Larsson, S. E., Ragnarsson, I. and Nilsson, S. G., Phys. Lett. **38B**, 269 (1972).
13. Götz, U., Pauli, H. C. and Junker, K., Phys. Lett. **39B**, 436 (1972).
14. Larsson, S. E. and Leander, G., Proc. Third IAEA Symposium on Physics and Chemistry of Fission, Rochester, 1973 (IAEA, Vienna, 1974) Paper IAEA-SM-174/06.
15. Nilsson, S. G., Tsang, C. F., Sobiczewski, A., Szymański, Z., Wycech, S., Gustafson, C., Lamm, I.-L., Möller, P. and Nilsson, B., Nucl. Phys. **A131**, 1 (1969).
16. Myers, W. D. and Swiatecki, W. J., Ann. of Phys. **55**, 395 (1969).
17. Randrup, J., Larsson, S. E., Möller, P., Sobiczewski, A. and Lukasiak, A., Contribution to this Symposium.
18. Krappe, H. J. and Nix, J. R., Proc. Third IAEA Symp. on Physics and Chemistry of Fission, Rochester, 1973 (IAEA, Vienna, 1974) Paper IAEA-SM-174/12.
19. Larsson, S. E., Leander, G., Ragnarsson, I. and Randrup, J., Contribution to this Symposium.

Department of Mathematical Physics
Lund Institute of Technology
P.O. Box 725
S-220 07 Lund 7, Sweden

Discussion

Question: H. J. Specht
One might naively expect that a nucleus like ^{20}Ne should show some tendency towards octupole deformation corresponding to $^{16}0+\alpha$. Do your calculations give any evidence for that?

Answer: S. G. Nilsson
Yes, the ground state of ^{20}Ne is in G. Leander's and S. E. Larsson's calculation ε_3-unstable. I interpret this theoretical result to give an indication that there should be low E3 vibrations near the ground state. However, the best situation for a stable secondary *minimum* occurs theoretically in ^{24}Mg, as was stated in the talk. The interacting orbitals have, for the ε-values relevant to that nucleus, come within closer proximity than in ^{20}Ne.

Comment: J. R. Huizenga
I would like to comment on the very interesting calculational result shown by S. G. Nilsson, where for the A region near thorium they observed a shallow lake or swimming pool between barriers 2 and 3. This type of potential landscape with barriers 2 and 3 being both asymmetric and much higher than barrier 1 is qualitatively in agreement with experimental evidence.

The low-energy photo-fission data for ^{232}Th requires that the higher barrier is asymmetric (in the present picture barriers 2 and 3) in order that the $1-$ and $2+$ states are degenerate as mentioned by H. Specht. This condition ensures an essentially constant ratio of quadrupole to dipole fission near and below the higher barrier. Although the photo-fission data is explainable without this shallow lake between barriers 2 and 3, there is also experimental evidence for a sharp resonance in the ^{230}Th (n,f) reaction with about 750 keV neutrons. It is this sharp resonance which is not explainable on the old barrier picture (where barriers 2 and 3 are a single barrier). The sharpness of this barrier at an energy near the top of the barrier requires a barrier landscape with a shallow lake as reported.

Question: H. J. Specht
Could you comment on the effect of the quadrupole pairing might have on level densities at the fission barrier?

Comment: S. G. Nilsson
The energy gap enters in a well-known way the level-density formula. It in turn is generally reduced at the barrier peaks with quadrupole pairing compared with the value obtained in the case of homogeneous pairing. The reason is that barrier peaks correspond to the crossing of levels of very different character (equatorial vs. polar orbitals). This is the average case. There are exceptions to this expected average. This is in particular true of the *second*-barrier region as shown by Larsson.

Comment: J. R. Nix
Of course, one could use an alternate potential that is closer to our expectation of what the nuclear potential really is, for example a Woods-Saxon potential or a Folded-Yukawa potential. Such a potential perhaps can be extrapolated to new regions of nuclei and deformation with more confidence than can a modified-oscillator potential.